

This document is confidential and is proprietary to the American Chemical Society and its authors. Do not copy or disclose without written permission. If you have received this item in error, notify the sender and delete all copies.

Biomimetic planar Polymer Membranes decorated with Enzymes as Functional Surfaces

Journal:	<i>Langmuir</i>
Manuscript ID	la-2018-00541g.R2
Manuscript Type:	Article
Date Submitted by the Author:	27-Jun-2018
Complete List of Authors:	Draghici, Camelia; University of Basel, Chemistry Department Mikhalevich, Viktoria; University of Basel, Department of Chemistry Gunkel-Grabole, Gesine; University of Basel, Department of Chemistry Kowal, Justyna; University of Basel, Department of Chemistry Meier, Wolfgang; University of Basel, Department of Chemistry Palivan, Cornelia; University of Basel, Chemistry Department

SCHOLARONE™
Manuscripts

1
2
3
4
5
6 **Biomimetic planar Polymer Membranes decorated with Enzymes as Functional Surfaces**
7
8
9
10

11
12 *Camelia Draghici^{a,b}‡, Viktoria Mikhalevich^a‡, Gesine Gunkel-Grabole^a, Justyna Kowal^a,*
13
14 *Wolfgang Meier^a, Cornelia G. Palivan^{a*}*
15
16
17
18
19

20 ^a Chemistry Department, University of Basel, Mattenstrasse 24a, BPR 1096 4002 Basel,
21
22 Switzerland
23
24

25 ^b Product Design, Mechatronics and Environment Department, Transilvania University of
26
27 Brasov, 29 Eroilor Blv, 500036 Brasov, Romania
28
29
30
31
32
33
34
35
36
37
38
39
40
41
42
43
44
45
46
47
48
49
50
51
52
53
54
55
56
57
58
59
60

ABSTRACT

Functional surfaces were generated by combination of enzymes with polymer membranes composed of an amphiphilic, asymmetric block copolymer poly(ethyleneglycol)-*block*-poly(γ -methyl- ϵ -caprolactone)-*block*-poly[(2-dimethylamino)ethylmethacrylate]. First, polymer films formed at air-water interface were transferred in different sequences onto silica solid support using the Langmuir–Blodgett technique, generating homogeneous monolayers and bilayers. Detailed characterization of these films provided insight into their properties (film thickness, wettability, topography and roughness). Based on these findings, the most promising membranes were selected for enzyme attachment. Functional surfaces were then generated by adsorption of two model enzymes that can convert phenol and its derivatives (laccase and tyrosinase), well known as high risk pollutants of drinking and natural water. Both enzymes preserved their activity upon immobilization with respect to their substrates. Depending on the properties of the polymer films, different degrees of enzymatic activity were observed: bilayers provided the best conditions both in terms of overall stability and enzymatic activity. The interaction between amphiphilic triblock copolymer films and enzymes is exploited to engineer “active surfaces” with specific functionalities and high efficacy resulting from the intrinsic activity of the biomolecules that is preserved by an appropriate synthetic environment.

KEYWORDS

Amphiphilic copolymers, Langmuir-Blodgett, hybrid membranes, bilayers, laccase activity, tyrosinase activity, sensing

INTRODUCTION

Nanoscience-based materials and systems offer solutions in a variety of fields such as medicine (drug delivery, diagnostics), catalysis, food- and environmental- sciences and technology. In particular, the combination of synthetic assemblies/membranes with active biomolecules (enzymes, proteins, mimics, nucleic acids) opens up exciting opportunities at the nanoscale such as confined spaces for complex reactions, serving as nanoreactors or artificial organelles, hybrid materials with stimuli-responsive properties, and “active surfaces”.¹⁻² In this respect, planar polymer membranes are ideal candidates to attach or insert biomolecules and obtain functional surfaces.³⁻⁴ They mimic the architecture of phospholipid bio-membranes but provide major advantages like increased mechanical stability, tunable membrane fluidity and thickness and induced stimuli-responsiveness depending on the polymer selected.⁵ Mono-, bi- and multilayer membranes on solid support were based on amphiphilic di- and triblock copolymers that can be generated by a variety of methods: surface-initiated polymerization, vesicle spreading or transfers from the air–water interface by the Langmuir-Blodgett (LB) or Langmuir-Schaefer techniques (LS).⁶ Such solid-supported membranes form thin polymer films that can be used for immobilization of biomolecules either directly by physical adsorption and chemical binding or by encapsulation or entrapment in different assemblies that are attached to the films.^{5, 7} Various enzymes, such as laccase, glucose oxidase, or horseradish peroxidase have been used to decorate synthetic thin polymer films.⁸⁻¹⁰ For example, physically adsorbed laccase on copolymer membranes was shown to have higher activity than free laccase in similar conditions, due to the protection by the polymer hydrophilic domain.⁸ Besides, polymer membranes served in various studies as matrices for transmembrane protein incorporation, indicating that polymer membranes are perfectly suitable for interactions with proteins.¹¹⁻¹³

1
2
3 Hybrid assemblies composed of enzymes and polymer membranes benefit from the intrinsic
4 biological activity of the enzymes and the stability of the polymer films, illustrating the potential
5 for applications, such as in production of specific compounds and for biosensing.⁵ A particularly
6 appealing field for applying protein-polymer membranes are the environmental sciences,
7 especially with respect to high water purity where the detection and removal of high risk
8 pollutants is a major challenge. Here, detection and removal of phenols and phenol derivatives is
9 of particular interest as the toxicity levels are usually in the range of 9-25 mg L⁻¹ for both
10 humans and aquatic life.¹⁴ Lipid films combined with laccase and tyrosinase served for phenol
11 biosensing,¹⁵⁻¹⁶ but polymeric films provide several advantages due to increased chemical and
12 mechanical stability.¹⁷⁻¹⁸ Yet, only very few studies provide fundamental insights into the
13 relationship between the molecular properties of the polymer films in relation to the overall
14 activity of the enzymes that is needed in order to design superior hybrid membranes for specific
15 applications.

16
17 Here, we focus on the formation of solid supported mono- and bilayer films of asymmetric
18 triblock copolymers, combine them with two enzymes (laccase and tyrosinase) typically used in
19 phenol biosensing¹⁵⁻¹⁶ and exploit their applicability as functional membranes. We systematically
20 modified the conditions of the combination of biomolecules and solid-supported synthetic
21 membranes in order to identify a stable environment for the enzymes that supports enzymatic
22 activity, providing detailed understanding of film properties required for functional surfaces that
23 can build effective biosensors for phenol derivative detection.

24
25 An asymmetric, amphiphilic triblock copolymer poly(ethyleneglycol)-*block*-poly(γ -methyl- ϵ -
26 caprolactone)-*block*-poly[(2-dimethylamino)ethylmethacrylate] (PEG₄₅-*b*-PMCL₁₀₁-*b*-
27 PDMAEMA₂₇, A₄₅-B₁₀₁-C₂₇) was selected for this study, because it forms uniform films with a

1
2
3 high degree of molecular ordering for attachment of laccase⁸ and with increased mechanical
4 stability.¹⁷⁻¹⁹ The two different hydrophilic blocks are composed of a protein repellent PEG
5
6 domain and a pH responsive PDMAEMA domain with tertiary amino groups that is expected to
7
8 aid adsorption of enzymes. This study goes beyond a previous study of laccase attachment on
9
10 PEG-*b*-PMCL-*b*-PDMAEMA monolayers,⁸ as it is focused on the accessibility of the
11
12 immobilized enzymes and the influence of molecular properties of the synthetic films on enzyme
13
14 immobilization. Various molecular and structural factors: (i) orientation of the asymmetric
15
16 amphiphilic ABC block copolymer at air-water interface; (ii) the parameters influencing the
17
18 mono- and bilayer film formation by the block copolymer at air-water interface and transfer to
19
20 silica solid support using the Langmuir–Blodgett technique; (iii) the structural properties, which
21
22 determine the block copolymer film formation and their availability for enzyme immobilization,
23
24 and (iv) the stability, accessibility and reactivity of the active surface of the enzyme-polymer
25
26 film were investigated. Different sequences of LB transfer resulting in different architectures
27
28 ranging from monolayers to bilayers were essential to evaluate the effect of the resulting
29
30 properties of these films and proteins entrapment on the overall functionality. The influence of
31
32 these factors serves to obtain a deep insight into the behavior of these hybrid enzyme-polymer
33
34 films, as an essential step towards generation of efficient and stable functional surfaces.
35
36
37
38
39
40
41
42
43

44 **MATERIALS AND METHODS**

45 **Materials.**

46
47 The amphiphilic asymmetric ABC block copolymer, poly(ethyleneglycol)-*block*-poly(γ -methyl-
48
49 ϵ -caprolactone)-*block*-poly[(2-dimethylamino)ethylmethacrylate], was synthesized as previously
50
51 described.²⁰ Polished silicon wafers were obtained from Si-Mat Silicon Materials, Germany.
52
53
54
55
56
57
58
59
60

1
2
3 Laccase from *Trametes versicolor*, tyrosinase from Mushroom (*Agaricus Bisporus*), 2,6-
4 dimethoxyphenol (DMP), 4-methoxyphenol (4-MP) and solvents (of highest purity grade) were
5 purchased from Sigma-Aldrich. The standard phosphate buffer saline solution (PBS), sodium
6 dodecyl sulfate (SDS) and 3-methyl-2-benzothiazolinone hydrazone (MBTH), Na₂HPO₄ 7 H₂O
7 and NaH₂PO₄ used to prepare the phosphate buffer were from Sigma-Aldrich. Bovine serum
8 albumin (BSA) was purchased from Thermo Fisher.
9

16 **Polymer Film Transfer on Solid Support.**

17
18
19 Polymer films were formed at the air-water interface by closing the LB barriers, which was
20 monitored as previously described by an EP³SW system (Nanofilm Technologie GmbH,
21 Göttingen, Germany) equipped with a Nd-YAG laser ($\lambda = 532$ nm), long distance objective
22 (Nikon, 20x) and monochrome CCD camera.⁸ The size of the Brewster angle microscopy (BAM)
23 image is 220 x 250 μm^2 , with a resolution of 1 μm . The transfer of the block copolymer films
24 onto the silica solid support was performed using the Langmuir-Blodgett (LB) technique,
25 following the previously described procedure using a Mini-trough (KSV Instruments, Finland).
26 In brief, the silica slides were cut into pieces of approx. 1 cm^2 and then cleaned by
27 ultrasonication in chloroform (three times, 15 minutes each time). For the “down” transfer, the
28 silica slides were placed in the air subphase, the polymer film was formed and transferred onto
29 the silica slide by dipping the LB dipper into the water. In order to avoid uncontrolled film
30 deposition or contamination the water surface was cleaned after “down” dipping transfer prior to
31 lifting the silica slides from the water subphase.
32
33
34
35
36
37
38
39
40
41
42
43
44
45
46
47
48

49 **Copolymer Monolayer and Bilayer Films Characterization.**

50
51 The dry thickness of the polymer monolayer and bilayer films were measured on two different
52 slides (at least five individual measurements on each) and average values with standard deviation
53
54
55
56
57
58
59
60

1
2
3 were calculated for values determined with a mean squared error (MSE) below 1. Film thickness
4 was measured with EP³SW imaging ellipsometer (Nanofilm Technologie GmbH, Göttingen,
5 Germany). The thickness of the silicon dioxide layer (~ 2 nm) was taken into account and
6 measurements were performed for ten incident angles ranging from 55° to 75°, with 1.5
7 refractive index value used for the polymer, using the nk_fix model. The wetting properties of
8 the polymer films were investigated with a contact angle goniometer, CAM 100 (LOT quantum
9 design) using a CDD camera with 50 mm optics. The measurements were performed by placing
10 droplets of ultrapure water with a micro-syringe on the solid supported films, images were then
11 recorded and analyzed by automatic curve fitting performed by the instrument software. The
12 drop volume was kept constant for all measurements, measurements were taken on two different
13 slides (five different areas on each) and average values and standard deviation were calculated. The
14 topography of the polymer films on silica slides was investigated by atomic force microscopy
15 (AFM) using a JPK NanoWizard® 3 AFM (JPK Instruments AG). All measurements were
16 carried out in the AC mode in air, using silicon cantilevers (PPP-NHCR, Nanosensors) with a
17 nominal spring constant of 10-130 N m⁻¹ and a resonance frequency of 300 kHz. The images
18 were analyzed with the data analysis software JPK Data Processing (v. 5.0).

40 **QCM Measurements of Enzyme Adsorption on Polymer Films.**

41
42 The adsorption of the enzymes on polymer films was studied with a quartz crystal microbalance
43 with dissipation (QCM-D) system Q-Sense E1 (Biolin Scientific, Sweden). The block copolymer
44 monolayer and bilayer films were first transferred to silicon dioxide QCM-D sensor chips (5
45 MHz quartz crystal q-sense, Biolin Scientific) by the LB technique using the mini-trough and
46 then placed in the QCM-D chamber. The QCM-D sensor was stabilized under buffer flow until
47 the frequency signal fluctuation was below ± 1 Hz. After system stabilization, solutions of 0.5 µg
48
49
50
51
52
53
54
55
56
57
58
59
60

1
2
3 mL⁻¹ laccase (in phosphate buffer, pH 7) or 0.5 μg mL⁻¹ tyrosinase (in PBS, pH 7) were
4 introduced into the QCM-D chamber with the flow speed of 100 μL min⁻¹. The enzyme was
5 allowed to adsorb for 1-2 hours until signal fluctuations were less than ± 1 Hz, incubated for
6 further 30 min before washing thoroughly with the appropriate buffer solution. The enzyme
7 adsorption and desorption stages (washing) are performed under the same constant slow flow
8 (100 μL min⁻¹) of enzyme solution and buffer, respectively, for several hours. The change in
9 resonance frequency value (Δf) measured with overtone 5 is used to calculate the mass (Δm)
10 adsorbed onto the polymer film, based on Sauerbrey equation (Δm = - CΔf, where C = 17.7 ng
11 cm⁻² Hz⁻¹ is a constant, depending on the quartz QCM-sensor properties.²¹

22 23 24 **Enzyme Adsorption on Polymer Films.**

25
26 Immobilization of enzymes on polymer films was performed after the film transfer onto the
27 solid support, in conditions similar to that used for the QCMD experiments (enzyme adsorption,
28 incubation and desorption). Silica slides with transferred mono- or bilayers of block copolymer
29 were immersed in enzyme solutions (0.5 μg mL⁻¹ for both laccase and tyrosinase, the first in in
30 phosphate buffer 50 mM, pH 7, the second in PBS buffer pH 7) for 2 h under shaking (dynamic
31 regime), incubation for 30 min without shaking (static regime), then rinsed with the buffer for 1
32 h (dynamic regime).

33 34 35 **Bicinchoninic Acid Assay.**

36
37 The concentrations of enzymes adsorbed on polymer films were determined by a bicinchoninic
38 acid assay (BCA assay, Micro BCA™ Protein Assay Thermo Fisher). Prior to the assay, the
39 enzymes were desorbed from the polymer films by incubation with sodium dodecyl sulfate
40 (SDS, 5 wt%) under shaking for 2 h, adapted from Gunkel et al.²² The enzyme concentration of
41 the supernatant solution was determined using a calibration curve obtained with bovine serum
42
43
44
45
46
47
48
49
50
51
52
53
54
55
56
57
58
59
60

1
2
3 abumin (BSA, 0.5–20 $\mu\text{g mL}^{-1}$). As the enzyme concentration in solution was 0.1–0.3 $\mu\text{g mL}^{-1}$,
4
5 the surface area was increased by using two silica plates with polymer films (8.75 cm^2/plate) for
6
7 one measurement. The amounts of desorbed proteins were quantified, calculating averages
8
9 determined with the two silica plates and from 4 repeated measurements.
10

11 **Activity of Free and Immobilized Enzymes.**

12
13
14 The enzymatic activity of laccase in solution (0.1–0.3 $\mu\text{g mL}^{-1}$) was studied using 2,6-
15
16 dimethoxyphenol (DMP) as substrate (0.1 mM DMP in 50 mM phosphate buffer, pH 7). DMP
17
18 forms an oxidation product that allows spectrophotometric detection at $\lambda_{\text{max}} = 470 \text{ nm}$.²³
19
20 Similarly, the laccase-polymer functionalized surfaces were placed into 24 well plates and a
21
22 solution of 0.1 mM DMP (in 50 mM phosphate buffer, pH 7) was added. Enzymatic activity was
23
24 monitored by spectrophotometric measurements of the supernatant solution. Four replicates of
25
26 different solid supported films were used. The activity of tyrosinase in solution (0.1–0.3 $\mu\text{g mL}^{-1}$)
27
28 was investigated spectrophotometrically with 0.2 mM 4-methoxyphenol (4-MP) as a substrate
29
30 and 2.5 mM 3-methyl-2-benzothiazolinone hydrazone hydrochloride (MBTH) as a dye at $\lambda_{\text{max}} =$
31
32 492 nm. The tyrosinase-polymer functionalized surfaces were placed into 24 well plates and a
33
34 solution of 0.2 mM 4-MP and 2.5 mM MBTH (in 50 mM phosphate buffer, pH 7) was added and
35
36 the activity was measured using the supernatant. For the calculation of the end concentration of
37
38 the product, the substrates (DMP and 4-MP, respectively) were reacted with an excess of the
39
40 enzyme (laccase and tyrosinase, 0.2 mg/ml). The product formation was monitored by UV-vis to
41
42 determine full conversion. Subsequently, the product solution was diluted to the concentrations
43
44 used in the calibration curve. For the calculation of enzyme activity, the wash solutions after
45
46 enzyme immobilization were collected and the activity was measured and subtracted from the
47
48 activity of the start solution. The difference was then assumed to be enzyme immobilized on the
49
50
51
52
53
54
55
56
57
58
59
60

1
2
3 surface and compared to measured activity of the immobilized enzymes. UV–Vis spectra were
4
5 recorded at $\lambda_{\max} = 492$ nm or $\lambda_{\max} = 470$ nm in the wavelength range 200–800 nm (with an
6
7 accuracy of 1 nm) using Quartz cuvettes on a Specord 210 Plus (analytik Jena Edition 2010) and
8
9 a Thermo Scientific NanoDrop 2000c.
10

11
12 All other reagents and methodologies are detailed in the text, figures legends or tables footnotes.
13
14

15 16 17 **RESULTS AND DISCUSSIONS**

18 19 **Formation of asymmetric polymer membranes on solid support.**

20
21 Planar polymer membranes on solid support were prepared with an amphiphilic asymmetric
22
23 ABC triblock copolymer PEG₄₅-*b*-PMCL₁₀₁-*b*-PDMAEMA₂₇, poly(ethyleneglycol)-*block*-
24
25 poly(γ -methyl- ϵ -caprolactone)-*block*-poly[(2-dimethylamino)ethylmethacrylate]. The
26
27 morphology and properties of the mono- and bilayer polymer membranes were investigated with
28
29 respect to their interaction with functional biomolecules.
30
31

32
33 The compression of polymer films at the air-water interface was monitored by Brewster angle
34
35 microscopy (BAM) before transferring the films on solid support by the Langmuir–Blodgett
36
37 technique as schematically illustrated in Figure 1. The transfer to silica slides was performed at
38
39 surface pressure (Π) values below the collapse pressure (26 mN m⁻¹). All polymer films were
40
41 obtained with a transfer ratio of about 1, indicating a transfer yield close to 100%, with uniform
42
43 deposition of the polymer onto the silica support. During Langmuir compression the copolymer
44
45 undergoes different phase transitions, starting with a “pancake” conformation (Figure 1.A),
46
47 followed by “mushroom” and “brush-like” arrangements, in which small lateral interactions
48
49 force the water soluble polymer blocks to coil (Figure 1 B, and E.a,b,c). At higher surface
50
51 pressures, the copolymers adopt a more ordered “cigar-like” conformation, and the final
52
53
54
55
56
57
58
59
60

1
2
3 conformation corresponds to a highly packed monolayer film formed at the collapse point Figure
4 1 C, and E.d).²⁴ To tune the interactions with enzymes, polymer films with different directions
5 and transfer sequences were prepared. Indeed, different directions and transfer sequences are
6 expected to induce formation of polymer films with different architectures, which will affect the
7 properties of these films and the resulting entrapment and accessibility of the enzymes. Different
8 transfer directions were used, “up” means the silicon substrate was moved up from the water
9 subphase to the air subphase and the inverse direction is called “down” transfer. The resulting
10 polymer films based on single transfers are labeled up and down, respectively, and combinations
11 of two transfers are labeled accordingly down-down, up-down, down-up or up-up (Figure 2.A).
12
13
14
15
16
17
18
19
20
21
22
23
24
25
26
27
28
29
30
31
32
33
34
35
36
37
38
39
40
41
42
43
44
45
46
47
48
49
50
51
52
53
54
55
56
57
58
59
60

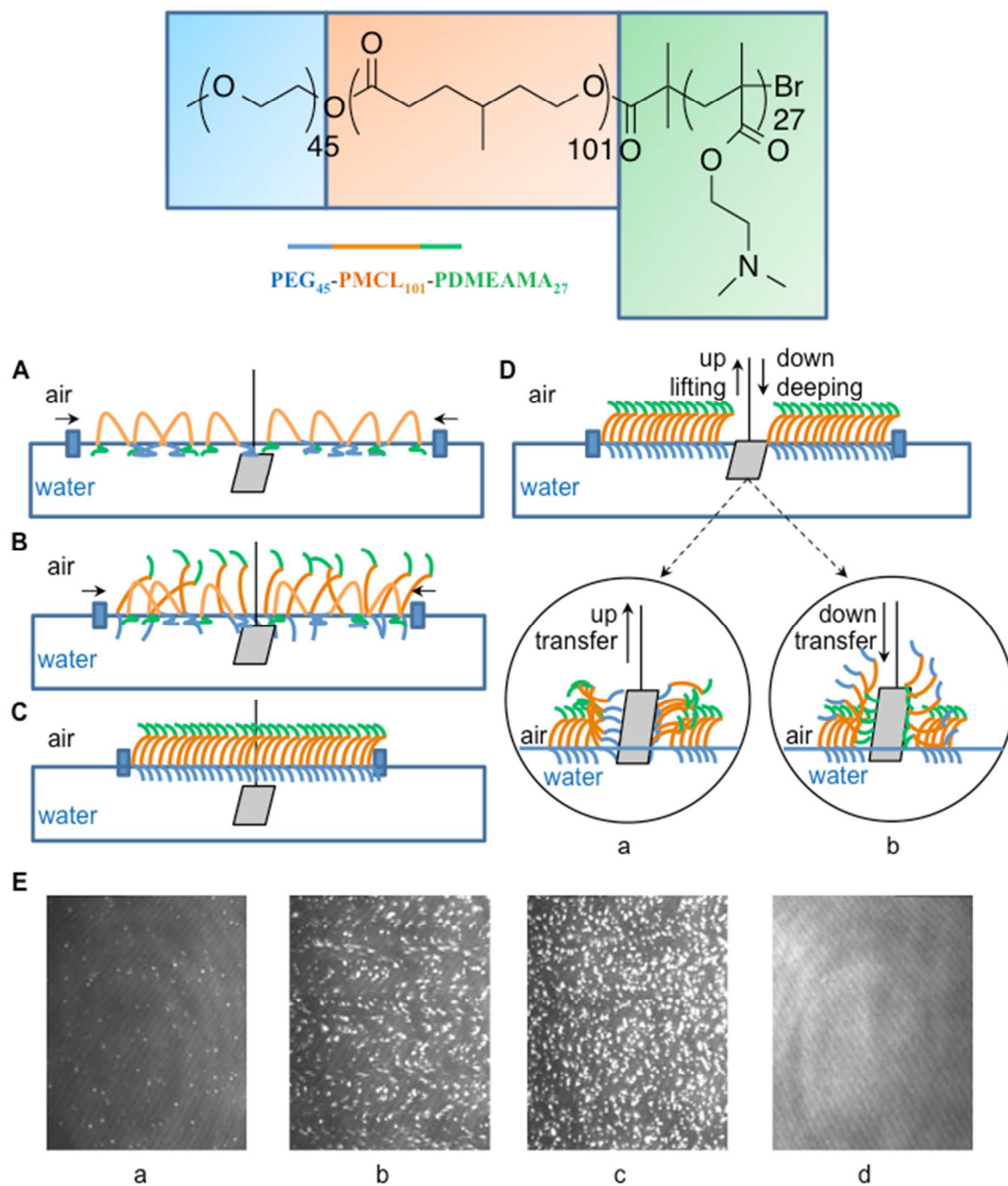


Figure 1. $\text{PEG}_{45}\text{-}b\text{-PMCL}_{101}\text{-}b\text{-PDMAEMA}_{27}$ copolymer used for solid supported membranes preparation. A to D – principle of the Langmuir–Blodgett transfer technique: A – polymer spread at air-water interface; B – polymer film organization at air-water interface; C – polymer film compressed at air-water interface; D – polymer transfer onto a hydrophilic solid support (a – up transfer, up lifting; b – down transfer, down dipping); E – Brewster angle

microscopy (BAM) images with the polymer film organization at air-water interface (a – “mushroom” conformation, at 12 mN m^{-1} ; b and c – “brush-like” arrangements at 15 mN m^{-1} and at 16 mN m^{-1} , respectively; d – uniform film formed at collapse point, 26 mN m^{-1}).

After compression, the polymer layers were transferred onto the silica slide, yielding solid supported polymer films. In the case of “up” transfer, the polished silica wafers were hooked on the dipper and placed in the water subphase before formation of the polymer layer at the air/water interface (Figure 1.D.a). For the “down” transfer, the silica slides were placed in the air subphase above the polymer layer (Figure 1.D.b). LB transfer technique allowed polymer film generation as monolayers or bilayers after two consecutive transfers (Figure 2.B).

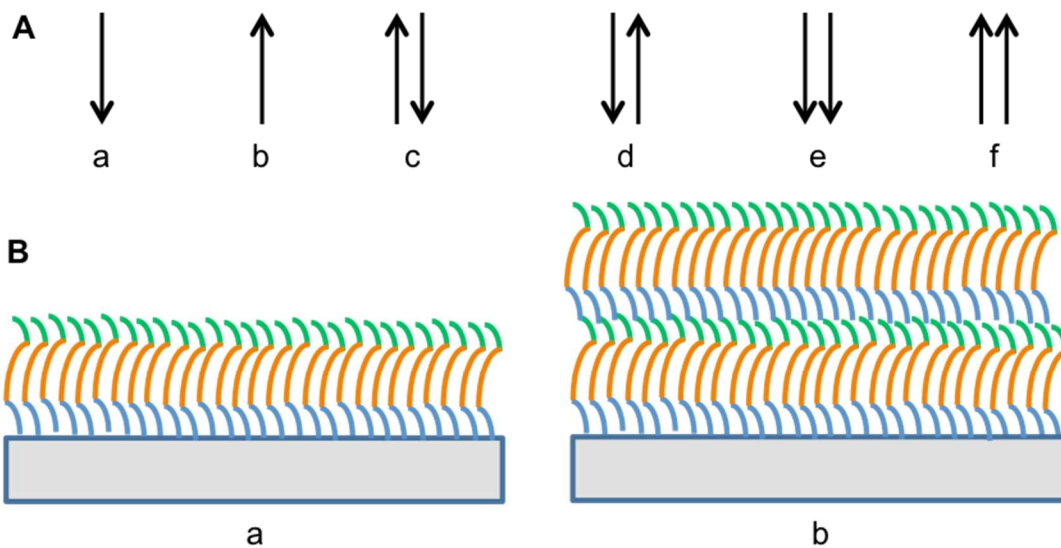


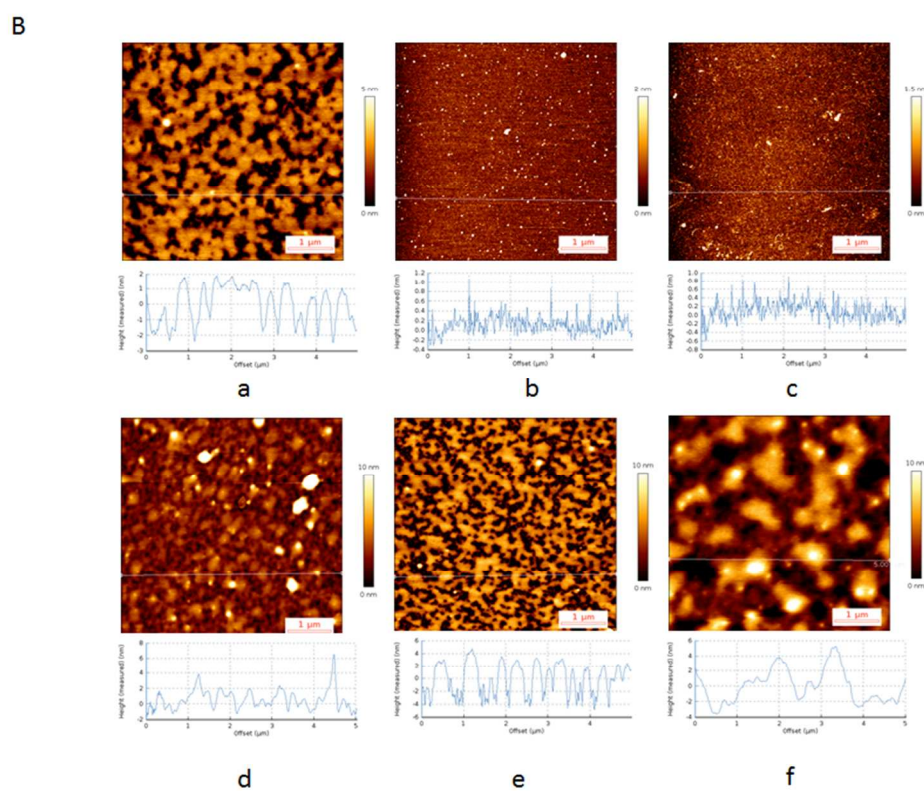
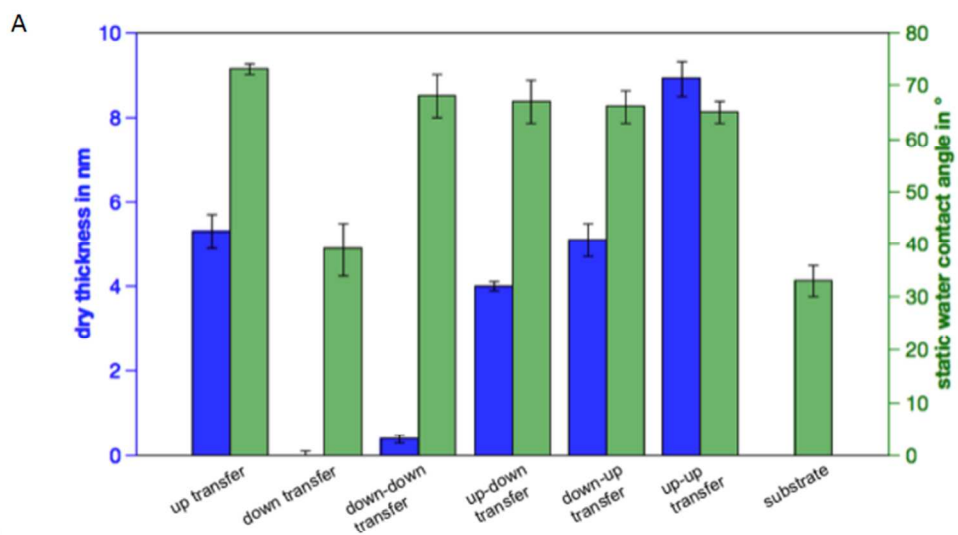
Figure 2. LB transfers to generate the polymer films: A – transfer directions (a – down transfer, down dipping; b – up transfer, up lifting; c – up-down transfer; d – down-up transfer; e – down-down transfer; f – up-up transfer); B – films resulting from specific transfers (a – monolayer film; b – bilayer film).

1
2
3 Earlier studies revealed that during “up” transfer the PEG block is adsorbed on the solid silica
4 surface and the PDMAEMA block is oriented outside.⁸ This equips the solid supported polymer
5 membranes with stimuli-responsive behaviour as PDMAEMA is pH responsive.²⁵ Additional
6 interesting properties are expected for bilayer morphologies, where the monolayer acts as a new
7 “substrate” for the second transfer, because it has been described that the interaction between
8 such films leads to considerable rearrangements.²⁶ Hence, a detailed insight into the morphology
9 of these mono- and bilayer polymer membranes is necessary in order to understand interaction of
10 the films with enzymes.
11
12

13
14
15 The thickness of the A₄₅-B₁₀₁-C₂₇ films is correlated with the number of layers and the type of
16 transfer and thus thickness measurements can indicate successful transfer of the polymer to the
17 substrate. The film thickness as determined by spectroscopic ellipsometry increased following
18 the order of polymer transfers on the solid support: down-down transfer < up-down transfer <
19 down-up transfer < up transfer (monolayer) < up-up transfer (bilayer) (Figure 3.A). In addition,
20 the surface hydrophilicity was determined to ensure favorable conditions for interaction between
21 enzymes and the A₄₅-B₁₀₁-C₂₇ block copolymer films. Static water contact angles (CA) for all
22 A₄₅-B₁₀₁-C₂₇ films are below 90° (Figure 3.A), therefore all polymer films on silica slides
23 possess a hydrophilic surface.²⁷ Further, these findings indicate that the triblock copolymer
24 chains are arranged at the air-water interface with a hydrophilic block oriented towards air.
25
26 Based on our previous results that showed that the C block is oriented to the air subphase in up
27 monolayers, it is deduced that the combined double transfers behave similarly and the
28 PDMAEMA block is oriented upwards.⁸ Moreover, the interaction of the polymer membranes
29 with the enzymes is also governed by the surface roughness (Figure 3.B), a high roughness
30 translates to a larger surface area available for interaction of biomolecules. The membrane
31
32
33
34
35
36
37
38
39
40
41
42
43
44
45
46
47
48
49
50
51
52
53
54
55
56
57
58
59
60

1
2
3 topography and the root mean square roughness (R_q) were determined by atomic force
4 microscopy measurements. R_q was selected as it is more sensitive to large deviations with
5 respect to the mean than other roughness parameters.²⁸ All polymer films except the down and
6 down-down transfer formed membranes of a few nanometers roughness, increasing with the
7 number and direction of Langmuir-Blodgett transfers (Table S1, Supporting Information). The
8 stability of the mono- and bilayer polymer membranes was evaluated by comparison of the film
9 topography of freshly prepared films with samples stored at room temperature in air for one
10 week and three months, respectively. (Figure S1, Supporting Information). Importantly, no
11 considerable topographical differences were detected for any of the transfer sequences,
12 underlining the long-term stability and the application potential as long-lived soft synthetic
13 surfaces.
14

15 The “up” transfer yielded a monolayer with a dry thickness of 5.3 ± 0.4 nm and a static water
16 contact angle (CA) value of $73 \pm 1^\circ$, which shows a clear change from a silica substrate ($33 \pm 3^\circ$)
17 (Figure 3). The surface roughness was 1.08 ± 0.04 nm (Table S1, Supporting Information). For
18 “down” and “down-down” transfers the data indicates that polymer membranes could not be
19 formed, the thickness was negligible ($0-0.4 \pm 0.1$ nm) and the contact angles were not
20 significantly different after “down” transfer ($39^\circ \pm 0.1^\circ$) compared to the bare silica substrate.
21 This may be explained by the orientation of the polymer chains, since both B and C blocks will
22 interact with the substrate (as opposed to the A block in “up” transfers). Hence, the interaction
23 with the substrate is governed by repulsion from the B block and attraction from the C block, and
24 it appears the repulsion was stronger than attractive forces and thus membranes could not be
25 formed.
26
27
28
29
30
31
32
33
34
35
36
37
38
39
40
41
42
43
44
45
46
47
48
49
50
51
52
53
54
55
56
57
58
59
60



1
2
3 **Figure 3.** Characterization of different solid supported A₄₅-B₁₀₁-C₂₇ copolymer films: A – thickness and wettability;
4 B – AFM images (AC mode in air) with different transfer types and their height profiles (a – up transfer, monolayer
5 film formed; b – down transfer, no film formation; c – down-down transfer, no film formation; d – down-up transfer,
6 down-up monolayer film formed; e – up-down transfer, up-down monolayer film formed; f – up-up transfer, bilayer
7 film formed).

8
9
10
11
12
13
14
15 Polymer films obtained after “up-down” and “down-up” transfers possess a dry thickness of
16
17 4.0 ± 0.1 nm and 5.1 ± 0.4 nm, respectively. These values are similar to the thickness of the
18
19 monolayer film, which suggests that a monolayer-based membrane was formed (up-down
20
21 monolayer and down-up monolayer). This further underlines that only an “up” transfer leads to a
22
23 successful membrane formation on silica support. However, the roughness of the membrane
24
25 increases (2.35 ± 0.07 nm for up-down monolayer), suggesting interaction or rearrangements of
26
27 the polymer membrane during a second transfer. Importantly, both up-down and down-up
28
29 monolayers possess a hydrophilic surface as confirmed by their CA values of $66 \pm 3^\circ$ and $67 \pm 4^\circ$
30
31 respectively. In the case of the “up-up” transfer, the film thickness is almost twice (8.9 ± 0.4 nm)
32
33 in comparison with the monolayer film, indicating formation of a bilayer membrane. This is
34
35 further supported by the membrane wettability ($65 \pm 2^\circ$) and an increase in roughness ($4.30 \pm$
36
37 0.48 nm).

38
39
40
41
42 We introduce the following terminology for the polymer membranes formed by the amphiphilic
43
44 asymmetric block copolymer based on the preparation method and the results discussed above:
45
46 monolayer for membranes prepared by “up” transfer, bilayer for “up-up” transfer, up-down
47
48 monolayer (“up-down”) and down-up monolayer (“down-up”). In contrary to z- and y-type lipid
49
50 films, this terminology describes the preparation more precisely and allows to relate the
51
52 preparation method directly with the interaction with the enzymes.²⁹
53
54
55
56
57
58
59
60

Adsorption of Enzyme on Copolymer Membranes.

The three most promising solid supported polymer membranes monolayer, up-down monolayer and bilayer were selected for further studies regarding adsorption of two different enzymes, laccase and tyrosinase. Laccase has a molecular weight of 96 kDa and dimensions of 4.5 nm × 5.5 nm × 6.5 nm,³⁰ while tyrosinase is larger with 120 kDa and is 10.4 nm x 10.45 nm x 10.84 nm in size.³¹ Enzyme adsorption on the different types of solid supported polymer membranes was investigated by quartz crystal microbalance (QCM-D) (Figure 4), as this method allows calculation of the mass of adsorbed enzyme on the membrane surface.

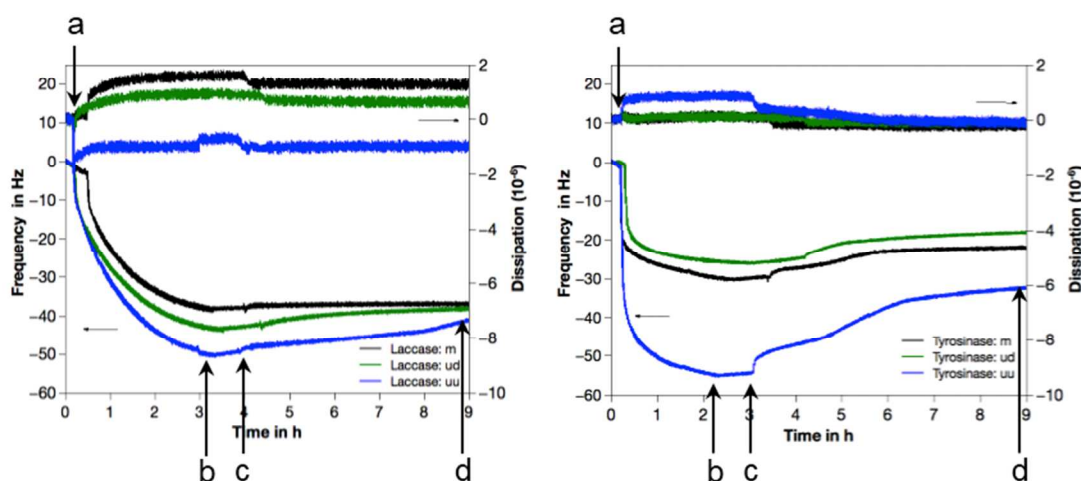


Figure 4. Changes in frequency (mass) and dissipation during the adsorption-incubation-desorption of laccase (left) and tyrosinase (right). Stages of enzymes adsorption: a – system stabilization (buffer flow); b – enzyme adsorption (enzyme flow); c – enzyme incubation (no flow); d – enzyme desorption (buffer flow). Both enzymes ($0.5 \mu\text{g mL}^{-1}$) adsorbed on polymer membranes: monolayer (m); up-down monolayer (ud) or bilayer (uu). QCM graphs shown are from the 5th overtone.

Our data was suitable for analysis with the Sauerbrey equation, as the change in dissipation was very small and the condition for dissipation (D) to frequency (F) ratio $\Delta D_n / (-\Delta F_n/n) \ll 4 \cdot 10^{-7} \text{ Hz}^{-1}$

1
2
3 ¹ is fulfilled (average value of $\sim 0.04 \cdot 10^{-7} \text{ Hz}^{-1}$, $n=5$, 5 MHz crystal).²¹ Hence, the frequency
4 difference is proportional to the adsorbed mass and the film is considered to be rigid.³²
5

6
7 We evaluated the changes in frequency (F) during the enzyme adsorption on different polymer
8 films in four stages as indicated by arrows in Figure 4: (a) system stabilization, with constant F
9 under buffer flow (10-20 minutes), (b) enzyme adsorption, F decreases under enzyme flow (2-3
10 hours), (c) enzyme incubation without flow, F almost constant (30 minutes), (d) enzyme
11 desorption, F increases under buffer flow until stable again, suggesting that no more enzyme is
12 desorbing. The adsorption of laccase on monolayer (up and up-down) and bilayer (up-up) films
13 occurred during 3 hours. After the incubation, less laccase was desorbed under buffer flow from
14 monolayers than from the bilayer (Figure S2, Supporting Information). No significant influence
15 of the film type on the deposited mass of laccase was observed, the enzyme was adsorbed on all
16 three types of polymer films in a range of $0.562\text{-}0.632 \mu\text{g cm}^{-2}$ (Figure 5, Table S2). Enzyme
17 molecular weights were taken into account to determine the surface coverage as $\Delta m/MW$ ratio,
18 and the number of enzymes adsorbed per area of polymer film.³³ For tyrosinase, adsorption
19 ended earlier (2 hours) and less enzyme was adsorbed on the monolayer films, whilst
20 considerably more was adsorbed on the bilayer film ($0.708 \mu\text{g cm}^{-2}$). After incubation, tyrosinase
21 desorption under buffer flow was more prominent than for laccase, thus at the end less tyrosinase
22 than laccase remained adsorbed on the films. The enzyme dimensions are expected to influence
23 the adsorption-desorption process. Indeed, a lower quantity of the larger enzyme tyrosinase, was
24 finally adsorbed on the polymer membrane surface, which may be explained by requiring more
25 space per molecule on the synthetic membrane.
26
27
28
29
30
31
32
33
34
35
36
37
38
39
40
41
42
43
44
45
46
47
48
49
50
51
52
53
54
55
56
57
58
59
60

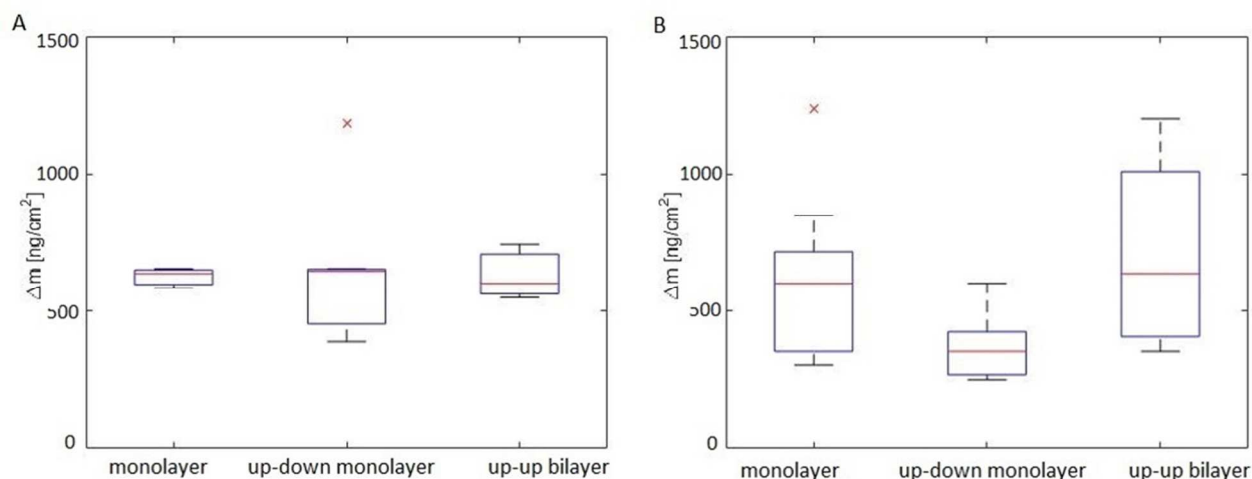


Figure 5. Amount of laccase (A) and tyrosinase (B) in ng/cm^2 calculated from QCM-D and shown in a boxplot with $n=3-6$.

Another factor affecting the enzyme immobilization process in the case of tyrosinase as compared to laccase is the tyrosinase tetramer structure, adopting a less compact configuration when adsorbing on the synthetic membrane.³¹ This explains why the type of polymer film (mono/bilayer film, up/down transfer) influenced the enzyme immobilization for tyrosinase more than for laccase. Our results are in agreement with studies where tyrosinase was deposited on lipid-based membranes prepared by Langmuir–Schaefer technique (horizontal lifting).¹⁷

The successful attachment of both enzymes on polymer films (monolayers and bilayer) is based on an electrostatic interaction between the enzymes and the exposed domain of the polymer films. PDMAEMA, which is the exposed C block of our polymer membranes, is positively charged at a pH between 5 and 8 due to protonation of the tertiary amino groups.³⁴ Both, laccase and tyrosinase are negatively charged in the pH range used, (laccase above pH 3.5³⁰ and tyrosinase above pH 4.7, Sigma – Datasheet). Hence, it is deduced that the electrostatic

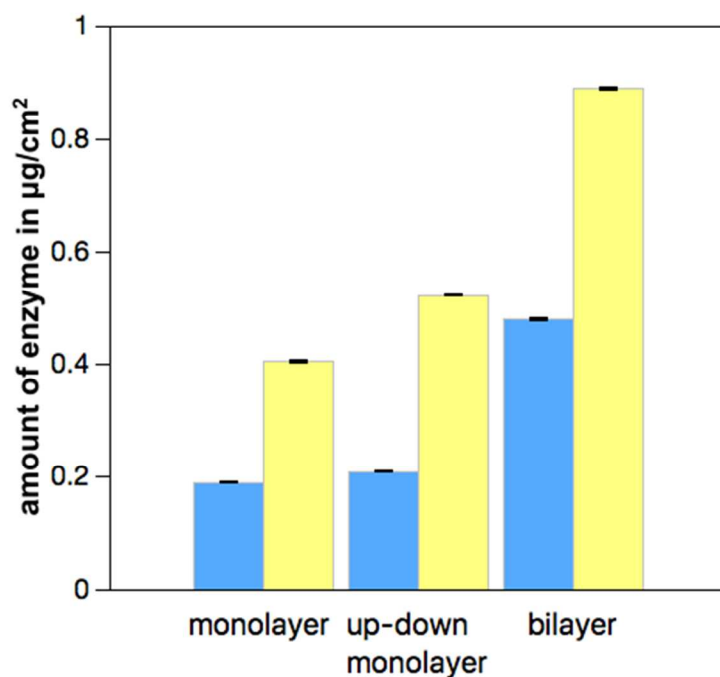
1
2
3 interaction is key to the adsorption of these enzymes on the synthetic mono- and bilayers. An
4 influence of the surface charge on the adsorption of laccase on positively charged methylene blue
5 self-assembled monolayer films has been observed in other studies as well.²³ The adsorption-
6 desorption behavior suggests that both adsorption and desorption of both enzymes differs with
7 the membrane type and enzyme. The adsorbed mass of laccase and tyrosinase on polymeric
8 membranes remained stable for at least 18 h (Figure S2, Supporting Information) at room
9 temperature.

19 **Active Surfaces Generation with Immobilized Enzymes on Copolymer Membranes.**

21 Enzyme adsorption on the polymer films for activity tests was performed by immersion of the
22 $A_{45}\text{-}B_{101}\text{-}C_{27}$ solid supported monolayer/bilayer films in enzyme solutions. AFM images of the
23 $A_{45}B_{101}C_{27}$ triblock copolymer films with adsorbed laccase and tyrosinase, respectively, did not
24 show significant differences when measured immediately, after 1 day and after 3 months (Figure
25 S3, Supporting Information). Long-term stability of these active surfaces supports their further
26 application and is discussed below.

35 In order to determine the amount of the enzymes immobilized on the $A_{45}\text{-}B_{101}\text{-}C_{27}$ solid
36 supported copolymer films, the bicinchoninic acid (BCA) assay was used. The BCA assay
37 allows to quantify the amount of proteins in solution, hence the enzymes were first desorbed
38 from the polymer films using SDS, contrary to the total enzyme amount adsorbed as determined
39 by QCM-D. The concentration of SDS (5 wt%) used for enzyme desorption was in the range
40 where the results obtained by the BCA assay are not affected, as stated by the supplier. The data
41 obtained with BCA assay for both enzymes is presented in Figure 6. In the case of laccase, the
42 amounts of desorbed enzyme available for BCA assay quantification are smaller than the amount
43 of adsorbed laccase, probably due to incomplete removal of the enzyme by SDS. This indicates

1
2
3 that not all laccase molecules are accessible, a fraction that cannot be removed remains
4 embedded in the polymer film.
5
6
7
8
9



10
11
12
13
14
15
16
17
18
19
20
21
22
23
24
25
26
27
28
29
30
31
32
33 **Figure 6.** Amounts of laccase (blue) and tyrosinase (yellow) removed from the monolayer, up-down monolayer and
34 bilayer polymer films, measured by BCA assay. The determined mass of the enzymes was expressed as mass per
35 surface area ($\mu\text{g cm}^{-2}$).
36
37
38
39

40
41 Interestingly, whilst the amount of immobilized laccase is approximately similar for all layer
42 types, as determined by QCM-D, the accessibility determined by the BCA assay varies with the
43 type of polymer film. Both monolayers (monolayer and up-down monolayer) have lower
44 concentrations of accessible laccase than the bilayer. For the monolayer films, the values of
45 removed laccase of $0.189 \pm 0.001 \mu\text{g cm}^{-2}$ (monolayer), and $0.209 \pm 0.001 \mu\text{g cm}^{-2}$ (up-down
46 monolayer) are significantly lower than what was obtained for the bilayer films (0.479 ± 0.003
47 $\mu\text{g cm}^{-2}$). A similar behavior has been observed for tyrosinase, with less enzyme detected in the
48
49
50
51
52
53
54
55
56
57
58
59
60

1
2
3 case of monolayers ($0.405 \pm 0.002 \mu\text{g cm}^{-2}$ for monolayer and $0.521 \pm 0.001 \mu\text{g cm}^{-2}$ for up-
4 down monolayer) than in the case of the bilayer ($0.888 \pm 0.001 \mu\text{g cm}^{-2}$). This observation can be
5 explained by a higher roughness and therefore a larger surface area of the bilayer, which makes
6 the immobilized biomolecules more accessible. A higher amount of tyrosinase was removed
7 according to the BCA assay compared to what was obtained by QCM-D. This unexpected
8 behavior might be related to differences in the adsorption-desorption procedures of these
9 methods and intrinsic properties of tyrosinase (conformation, charge, interaction with the
10 synthetic membrane). Besides, the measurement principles are very different and for the BCA
11 assay also affected by the accessibility of the enzymes, complicating an immediate comparison.
12 Importantly, both QCM-D and BCA assay confirm that laccase and tyrosinase adsorb on the
13 different types of polymer films, a prerequisite for the development of a biosensors based on the
14 specific enzyme activities. .

30 **Enzymatic Activity on Polymer Membranes.**

31
32
33 The enzymatic activity of laccase and tyrosinase adsorbed on polymer monolayer and bilayer
34 membranes was studied and compared with the activity of free enzymes. The activities were
35 studied with phenol derivatives as models to assess the biodetection of phenols by our active
36 surfaces, 2,6-dimethoxyphenol (DMP, 0.1 mM) in the case of laccase and 4-methoxyphenol (4-
37 MP, 0.2 mM) for tyrosinase. The activity of both enzymes free in solution increased with the
38 enzyme concentration ($0.1\text{-}0.3 \mu\text{g mL}^{-1}$) (Figure S4, Table S3, Supporting Information) and
39 maximum activity of laccase free in solution was reached after 24 h, while tyrosinase free in
40 solution reached a maximum after 1 h. Therefore, the activity of the immobilized enzymes on the
41 copolymer mono- and bilayer films was tested for different time periods, laccase for 24 h (with
42 maximum activity at 19-24 h) and tyrosinase for 6 h (with maximum activity at 2-3 h). The
43
44
45
46
47
48
49
50
51
52
53
54
55
56
57
58
59
60

1
2
3 activity increased starting from enzymes immobilized on monolayer to up-down monolayer, with
4
5 the enzymes immobilized on bilayer showing the highest activity (Figure 7 A, B, Figure S5
6
7 Supporting Information). Thereby, for laccase the maximum concentration for the product was
8
9 detected after 24h on the bilayer ($1.05 \pm 0.55 \mu\text{M}$), compared to the monolayer, where the
10
11 maximum was after 19 h ($0.39 \pm 0.26 \mu\text{M}$). For tyrosinase the highest concentration of formed
12
13 product on the monolayer was detected after 4h ($21.33 \pm 7.35 \mu\text{M}$) and for the bilayer after 2h
14
15 ($35.38 \pm 6.09 \mu\text{M}$) (Figure S6, Table S4 Supporting Information). In literature these reactions are
16
17 well known and the mechanisms described.³⁵⁻³⁶ This activity behavior correlated well with the
18
19 concentration of accessible enzymes on the bilayer film as determined by BCA assay. As the
20
21 highest activity of laccase and tyrosinase has been obtained for the enzymes immobilized on
22
23 bilayer, we used the bilayer films to get more insight into the the phenol derivative detection
24
25 range by decreasing 10-fold the concentration of the enzymes substrate (Figure 7 C). The
26
27 autooxidation of the enzyme substrates has been taken into account as a background correction,
28
29 that has been performed for all curves by subtraction of the absorption intensity obtained when
30
31 the enzyme substrate was added to the polymer membrane. The 10-fold decrease of the enzyme
32
33 substrates concentration decreased the enzymatic activity only slightly, indicating that lower
34
35 concentrations of phenol derivatives can be efficiently detected by our functional surfaces (with
36
37 0.01 mM laccase substrate concentration and 0.02 mM tyrosinase substrate concentration).
38
39 Importantly, the concentration of remaining substrate, which acts as a model for phenol
40
41 contaminants, is reduced by 50% for tyrosinase and 10% for laccase. This further highlights the
42
43 potential of the hybrid membranes for sensing and detection applications.
44
45
46
47
48
49
50
51
52
53
54
55
56
57
58
59
60

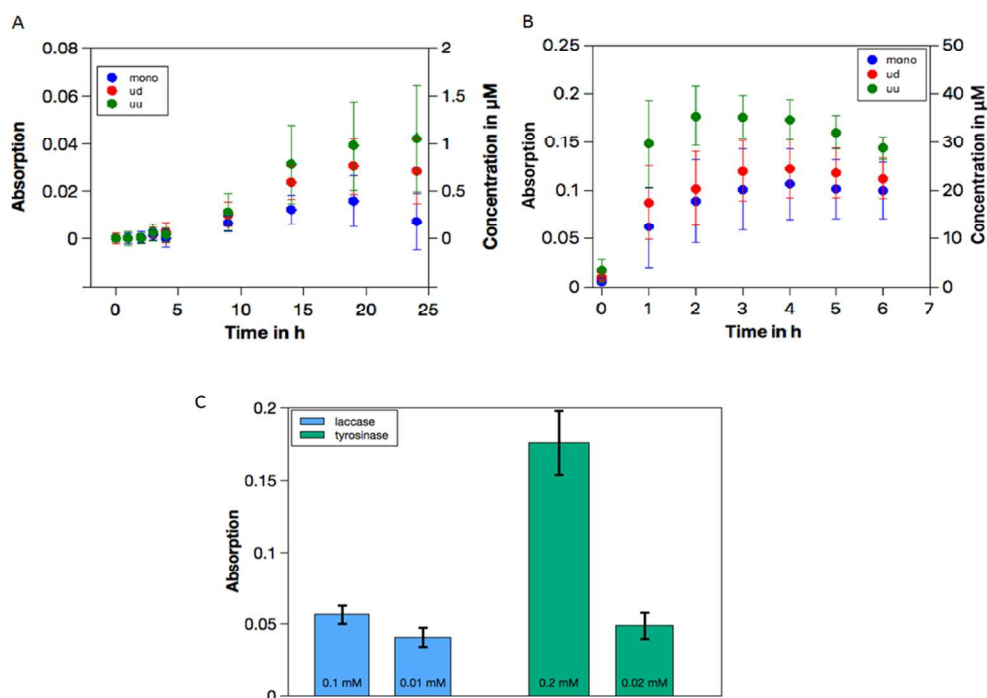


Figure 7. Activity of enzymes immobilized on the A₄₅-B₁₀₁-C₂₇ block copolymer films as determined by oxidative product formation. (A) Laccase with 0.1 mM DMP as substrate which forms a product with a characteristic UV/vis absorption ($\lambda = 470$) (A), and (B) tyrosinase with 0.2 mM 4-MP as substrate forming a product that can be detected by UV/vis absorption at $\lambda = 492$). Curves are based on: monolayer (m, blue), up-down monolayer (ud, red), bilayer (uu, green), (lines added to guide the eye only). Activity of tyrosinase and laccase immobilized on the bilayer (uu) for two different concentrations of the enzyme substrates (C): DMP 0.1 mM and 0.01 mM (after 24 h), and 4-MP 0.2 mM and 0.02 mM (after 3 h). Enzymatic activity is shown via absorption intensity as measured and product concentration (μM) as calculated using the calibration curves in Figure S6. For all measurements, background correction has been performed by subtraction of the absorption intensity obtained when the enzyme substrate was added to the polymer membrane.

Enzymes immobilized on an up-down monolayer resulted in a more active surface than the monolayer. Different parameters may account for these differences in behavior, it may be related

1
2
3 to the different roughness of these films, which affects the accesibility of the enzymes. In
4
5 addition, different enzyme conformations resulting in reduced conformational freedom of the
6
7 enzyme that are affecting the mode of interaction between the enzyme and substrate may also
8
9 affect the enzyme activity on the polymeric membranes. Importantly, both laccase and tyrosinase
10
11 remained active upon adsorption on the polymer films as indicated by the increase in absorption.
12
13 Yet, compared to free enzyme in solution the adsorbed enzymes have lower activity, which
14
15 might be related to various molecular factors, as for example to the reduced accesibility of
16
17 adsorbed enzymes or reduced conformational freedom of the enzyme. The stability of the films
18
19 has been evaluated by preparing them two weeks and one day before the enzyme immobilization,
20
21 respectively. As the activity for both laccase and tyrosinase did not change, it indicates that the
22
23 films preserve their properties up to two weeks (Figure S7, Supporting Information). The
24
25 measured activity was compared with the activity that is theoretically expected if the enzyme is
26
27 fully accesible to the substrates (Figure S8, Supporting Information). The theoretically expected
28
29 and measured activity are very similar for tyrosinase immobilized on the bilayer polymer film
30
31 (up-up). For laccase, however, the measured activity is clearly lower than what would be
32
33 expected based on the amount of immobilized enzyme. This behavior is indicating a reduced
34
35 accesibility of the enzyme after imobilization. Importantly, a comparison with surfaces that are
36
37 not functionalized with polymer membranes.further underlines the advantageous effect of the
38
39 polymers as there is hardly any enzymatic activity observed on bare silica despite a higher
40
41 amount of adsorbed enzyme.
42
43
44
45
46
47
48

49 Together, the stability of the solid supported copolymer films and the preserved bioactivity
50
51 indicate that these active surfaces have high potential upon optimization, for phenol and phenol
52
53 derivatives biosensing.
54
55
56
57
58
59
60

CONCLUSIONS

The advantageous combination of the intrinsic bio-activity of the enzymes with the robustness and versatility of solid supported polymer membranes allows production of efficient “active surfaces”. In this respect, a systematic analysis of the effects of the molecular factors of the polymer membranes on the activity of the enzymes represents a crucial step that is necessary to control the efficacy of such functional planar membranes and advance their development for production of desired compounds or for biosensing. We reported here polymer membranes that provide a stable, solid-supported environment for the enzymes. Interaction of both enzymes with different arrangements of the polymer films produced by LB transfer: mono- and bilayers with different morphology and properties (film thickness, wettability and roughness) were investigated. The three most promising polymer films (the monolayer, the up-down monolayer and the bilayer) were selected for enzyme adsorption and activity studies. It was observed that enzyme adsorption on the polymeric film is affected more by electrostatic interactions at enzyme/polymer interface than by surface roughness. Whilst both, laccase and tyrosinase preserved their enzymatic activity upon adsorption on the different types of polymer films, their activity was affected by the type of polymer film: bilayer films showed the highest activity for both enzymes. Therefore, bilayers are the most appealing candidates for combination with enzymes to sustain enzymatic reaction for sensing applications in aqueous environments. However, in order to advance towards potential applications of such functional planar bio-hybrid membranes further optimization is necessary to support scale-up as biosensors for detection of phenol and its harmful derivatives, well known as pollutants of drinking and natural water.

1
2
3 ASSOCIATED CONTENT
4

5 Supporting Information: Characterization of the polymer films; AFM; roughness of synthetic
6 films; QCM-D frequency changes; Adsorption of enzymes on synthetic films; Activity of the
7 free laccase and tyrosinase; Absorption curves for tyrosinase and laccase on bilayer; Calibration
8 curves for enzymatic product; Activity of the enzymes on bilayer two weeks after preparation;
9
10 Relative enzymatic activity.
11
12
13
14
15
16
17
18
19

20 AUTHOR INFORMATION
21

22 **Corresponding Author**
23

24 *CGP, E-mail: cornelia.palivan@unibas.ch
25
26

27 **Author Contributions**
28

29
30 ‡ CD and VM contributed equally to this work.
31
32
33
34

35 ACKNOWLEDGMENT
36

37 Financial support was provided by the Swiss National Foundation (SNF), the National
38 Centre of Competence Molecular System Engineering (NCCR MSE) and the University
39 of Basel, and this is gratefully acknowledged. CD acknowledges the financial support
40 from the Swiss National Science Foundation, International Short Visit (IZK0Z2_150884).
41
42 We would like to thank Prof. Patrick Shahgaldian and Mina Moradi for access to the
43
44
45
46
47
48
49
50
51
52
53
54
55
56
57
58
59
60

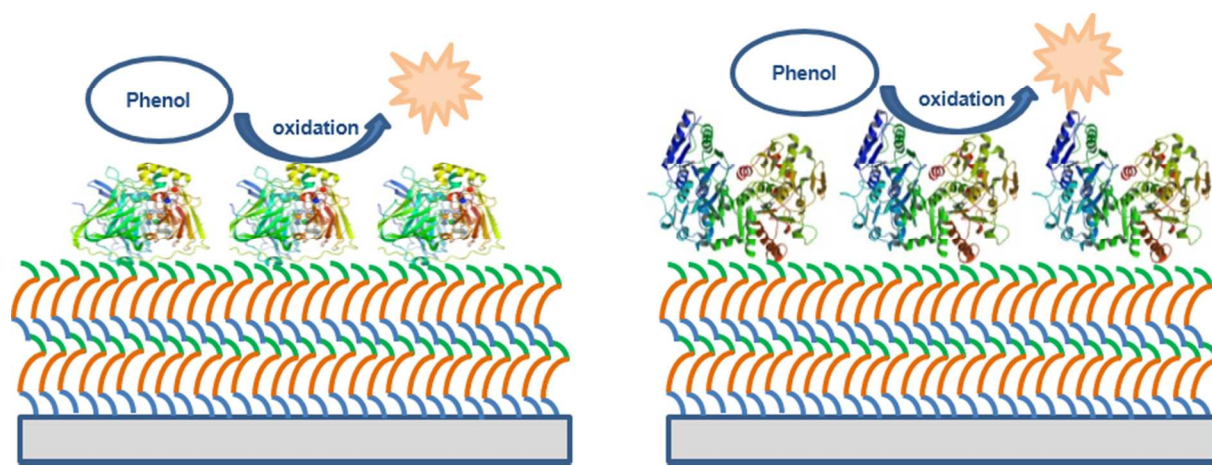
REFERENCES

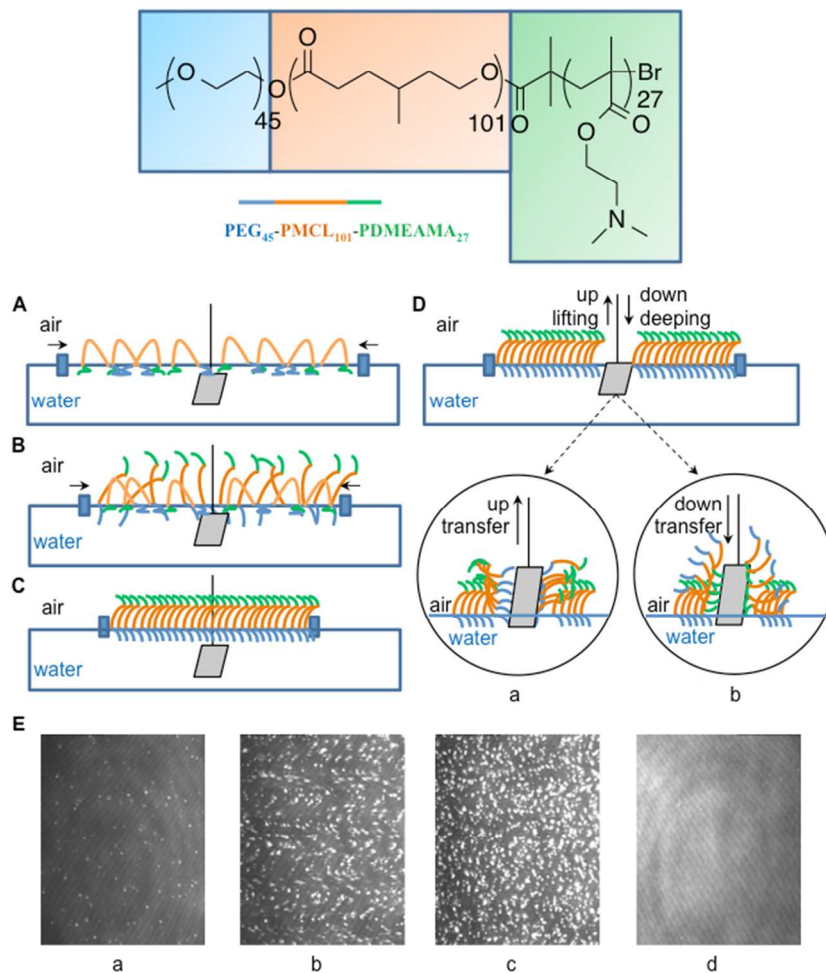
1. Küchler, A.; Yoshimoto, M.; Luginbühl, S.; Mavelli, F.; Walde, P., Enzymatic reactions in confined environments. *Nat. Nanotechnol.* **2016**, *11*, 409.
2. Biju, V., Chemical modifications and bioconjugate reactions of nanomaterials for sensing, imaging, drug delivery and therapy. *Chem. Soc. Rev.* **2014**, *43* (3), 744-764.
3. Gunkel-Grabole, G.; Sigg, S.; Lomora, M.; Lorcher, S.; Palivan, C. G.; Meier, W. P., Polymeric 3D nano-architectures for transport and delivery of therapeutically relevant biomacromolecules. *Biomater. Sci.* **2015**, *3* (1), 25-40.
4. Palivan, C. G.; Goers, R.; Najer, A.; Zhang, X.; Car, A.; Meier, W., Bioinspired polymer vesicles and membranes for biological and medical applications. *Chem. Soc. Rev.* **2016**, *45* (2), 377-411.
5. Garni, M.; Thamboo, S.; Schoenenberger, C.-A.; Palivan, C. G., Biopores/membrane proteins in synthetic polymer membranes. *Biochim. Biophys. Acta, Biomembr.* **2017**, *1859* (4), 619-638.
6. Kowal, J.; Zhang, X.; Dinu, I. A.; Palivan, C. G.; Meier, W., Planar Biomimetic Membranes Based on Amphiphilic Block Copolymers. *ACS Macro Lett.* **2014**, *3* (1), 59-63.
7. Hartmann, M.; Jung, D., Biocatalysis with enzymes immobilized on mesoporous hosts: the status quo and future trends. *J. Mater. Chem.* **2010**, *20* (5), 844-857.
8. Draghici, C.; Kowal, J.; Darjan, A.; Meier, W.; Palivan, C. G., "Active Surfaces" Formed by Immobilization of Enzymes on Solid-Supported Polymer Membranes. *Langmuir* **2014**, *30* (39), 11660-11669.
9. Welch, M. E.; Doublet, T.; Bernard, C.; Malliaras, G. G.; Ober, C. K., A glucose sensor via stable immobilization of the GOx enzyme on an organic transistor using a polymer brush. *J. Polym. Sci., Part A: Polym. Chem.* **2015**, *53* (2), 372-377.
10. Lane, S. M.; Kuang, Z.; Yom, J.; Arifuzzaman, S.; Genzer, J.; Farmer, B.; Naik, R.; Vaia, R. A., Poly (2-hydroxyethyl methacrylate) for enzyme immobilization: impact on activity and stability of horseradish peroxidase. *Biomacromolecules* **2011**, *12* (5), 1822-1830.
11. Kowal, J. Ł.; Kowal, J. K.; Wu, D.; Stahlberg, H.; Palivan, C. G.; Meier, W. P., Functional surface engineering by nucleotide-modulated potassium channel insertion into polymer membranes attached to solid supports. *Biomaterials* **2014**, *35* (26), 7286-7294.
12. Zhang, X.; Fu, W.; Palivan, C. G.; Meier, W., Natural channel protein inserts and functions in a completely artificial, solid-supported bilayer membrane. *Sci. rep.* **2013**, *3*, 1-7.
13. Lomora, M.; Gunkel-Grabole, G.; Mantri, S.; Palivan, C. G., Bio-catalytic nanocompartments for in situ production of glucose-6-phosphate. *Chem. Commun.* **2017**, *53* (73), 10148-10151.
14. Villegas, L. G. C.; Mashhadi, N.; Chen, M.; Mukherjee, D.; Taylor, K. E.; Biswas, N., A Short Review of Techniques for Phenol Removal from Wastewater. *Curr. Pollut. Rep.* **2016**, *2* (3), 157-167.
15. Cabaj, J.; Sołoducho, J.; Chyla, A.; Bryjak, J.; Zynek, K., The characterization of ordered thin films built of immobilized phenoloxidases. *Sens. Actuators, B* **2009**, *136* (2), 425-431.
16. Cabaj, J.; Sołoducho, J.; Nowakowska-Oleksy, A., Langmuir–Blodgett film based biosensor for estimation of phenol derivatives. *Sens. Actuators, B* **2010**, *143* (2), 508-515.
17. Cabaj, J.; Sołoducho, J.; Świst, A., Active Langmuir–Schaefer films of tyrosinase—Characteristic. *Sens. Actuators, B* **2010**, *150* (2), 505-512.

18. Böyükbayram, A. E.; Kıralp, S.; Toppare, L.; Yağcı, Y., Preparation of biosensors by immobilization of polyphenol oxidase in conducting copolymers and their use in determination of phenolic compounds in red wine. *Bioelectrochemistry* **2006**, *69* (2), 164-171.
19. Ameer, Q.; Adeloju, S. B., Development of a potentiometric catechol biosensor by entrapment of tyrosinase within polypyrrole film. *Sens. Actuators, B* **2009**, *140* (1), 5-11.
20. Matter, Y.; Enea, R.; Casse, O.; Lee, C. C.; Baryza, J.; Meier, W., Amphiphilic PEG-b-PMCL-b-PDMAEMA Triblock Copolymers: From Synthesis to Physico-Chemistry of Self-Assembled Structures. *Macromol. Chem. Phys.* **2011**, *212* (9), 937-949.
21. Vogt, B. D.; Lin, E. K.; Wu, W.-I.; White, C. C., Effect of Film Thickness on the Validity of the Sauerbrey Equation for Hydrated Polyelectrolyte Films. *J. Phys. Chem. B* **2004**, *108* (34), 12685-12690.
22. Gunkel, G.; Huck, W. T. S., Cooperative Adsorption of Lipoprotein Phospholipids, Triglycerides, and Cholesteryl Esters Are a Key Factor in Nonspecific Adsorption from Blood Plasma to Antifouling Polymer Surfaces. *J. Am. Chem. Soc.* **2013**, *135* (18), 7047-7052.
23. Qiu, H.; Xu, C.; Huang, X.; Ding, Y.; Qu, Y.; Gao, P., Immobilization of Laccase on Nanoporous Gold: Comparative Studies on the Immobilization Strategies and the Particle Size Effects. *J. Phys. Chem. C* **2009**, *113* (6), 2521-2525.
24. Haefele, T.; Kita-Tokarczyk, K.; Meier, W., Phase Behavior of Mixed Langmuir Monolayers from Amphiphilic Block Copolymers and an Antimicrobial Peptide. *Langmuir* **2006**, *22* (3), 1164-1172.
25. Vasquez, D.; Einfalt, T.; Meier, W.; Palivan, C. G., Asymmetric Triblock Copolymer Nanocarriers for Controlled Localization and pH-Sensitive Release of Proteins. *Langmuir* **2016**, *32* (40), 10235-10243.
26. Kita-Tokarczyk, K.; Junginger, M.; Belegriou, S.; Taubert, A., Amphiphilic Polymers at Interfaces. In *Self Organized Nanostructures of Amphiphilic Block Copolymers II*, Müller, A. H. E.; Borisov, O., Eds. Springer Berlin Heidelberg: Berlin, Heidelberg, 2011; pp 151-201.
27. Förch, R.; Schönherr, H.; Jenkins, A. T. A., *Surface design: applications in bioscience and nanotechnology*. John Wiley & Sons: 2009.
28. Raposo, M.; Ferreira, Q.; Ribeiro, P., A guide for atomic force microscopy analysis of soft-condensed matter. *Modern research and educational topics in microscopy* **2007**, *1*, 758-769.
29. Girard-Egrot, A. P.; Godoy, S.; Blum, L. J., Enzyme association with lipidic Langmuir–Blodgett films: Interests and applications in nanobioscience. *Adv. Colloid Interface Sci.* **2005**, *116* (1), 205-225.
30. Piontek, K.; Antorini, M.; Choinowski, T., Crystal Structure of a Laccase from the Fungus *Trametes versicolor* at 1.90-Å Resolution Containing a Full Complement of Coppers. *J. Biol. Chem.* **2002**, *277* (40), 37663-37669.
31. Ismaya, W. T.; Rozeboom, H. J.; Weijn, A.; Mes, J. J.; Fusetti, F.; Wichers, H. J.; Dijkstra, B. W., Crystal Structure of *Agaricus bisporus* Mushroom Tyrosinase: Identity of the Tetramer Subunits and Interaction with Tropolone. *Biochemistry* **2011**, *50* (24), 5477-5486.
32. Reviakine, I.; Johannsmann, D.; Richter, R. P., Hearing What You Cannot See and Visualizing What You Hear: Interpreting Quartz Crystal Microbalance Data from Solvated Interfaces. *Anal. Chem.* **2011**, *83* (23), 8838-8848.
33. Mazur, M.; Krysiński, P.; Michota-Kamińska, A.; Bukowska, J.; Rogalski, J.; Blanchard, G. J., Immobilization of laccase on gold, silver and indium tin oxide by zirconium–phosphonate–carboxylate (ZPC) coordination chemistry. *Bioelectrochemistry* **2007**, *71* (1), 15-22.

- 1
2
3 34. Mahltig, B.; Gohy, J.-F.; Antoun, S.; Jérôme, R.; Stamm, M., Adsorption and structure
4 formation of the weak polyelectrolytic diblock copolymer, PVP-b-PDMAEMA. *Colloid Polym.*
5 *Sci.* **2002**, *280* (6), 495-502.
6
7 35. Espín, J. C.; varon-castellanos, R.; Tudela, J.; Canovas, G., *Kinetic study of the oxidation*
8 *of 4-hydroxyanisole catalyzed by tyrosinase.* 1997; Vol. 41, p 1265-76.
9 36. Kudanga, T.; Nemadziva, B.; Le Roes-Hill, M., Laccase catalysis for the synthesis of
10 bioactive compounds. *Appl. Microbiol. Biotechnol.* **2017**, *101* (1), 13-33.
11
12
13
14
15
16
17
18
19
20
21
22
23
24
25
26
27
28
29
30
31
32
33
34
35
36
37
38
39
40
41
42
43
44
45
46
47
48
49
50
51
52
53
54
55
56
57
58
59
60

TOC Graphic





45
46
47
48
49
50
51
52
53
54
55
56
57
58
59
60

Figure 1. PEG₄₅-b-PMCL₁₀₁-b-PDMEAMA₂₇ copolymer used for solid supported membranes preparation. A to D – principle of the Langmuir–Blodgett transfer technique: A – polymer spread at air-water interface; B – polymer film organization at air-water interface; C – polymer film compressed at air-water interface; D – polymer transfer onto a hydrophilic solid support (a – up transfer, up lifting; b – down transfer, down dipping); E – BAM images with the polymer film organization at air-water interface (a – “mushroom” conformation, at 12 mN m⁻¹; b and c – “brush-like” arrangements at 15 mN m⁻¹ and at 16 mN m⁻¹, respectively; d – uniform film formed at collapse point, 26 mN m⁻¹).

254x338mm (72 x 72 DPI)

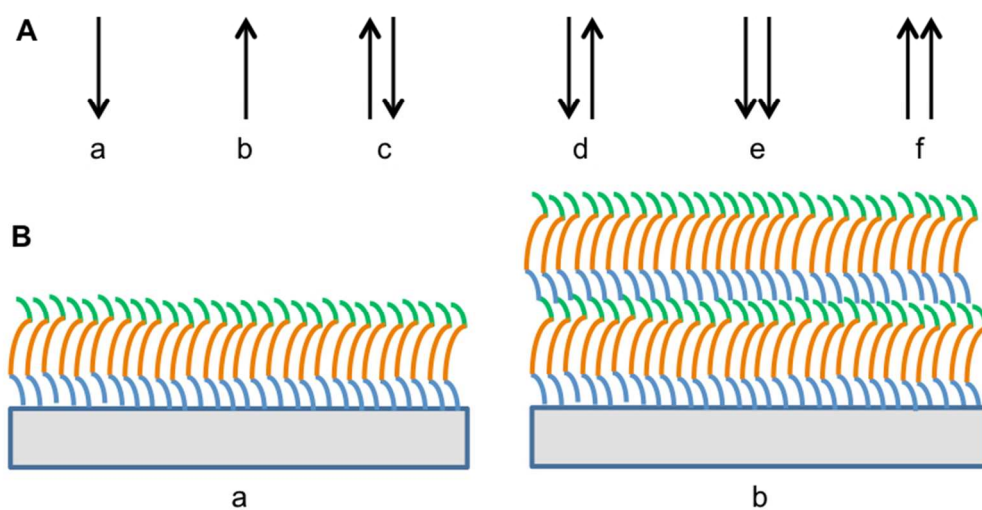
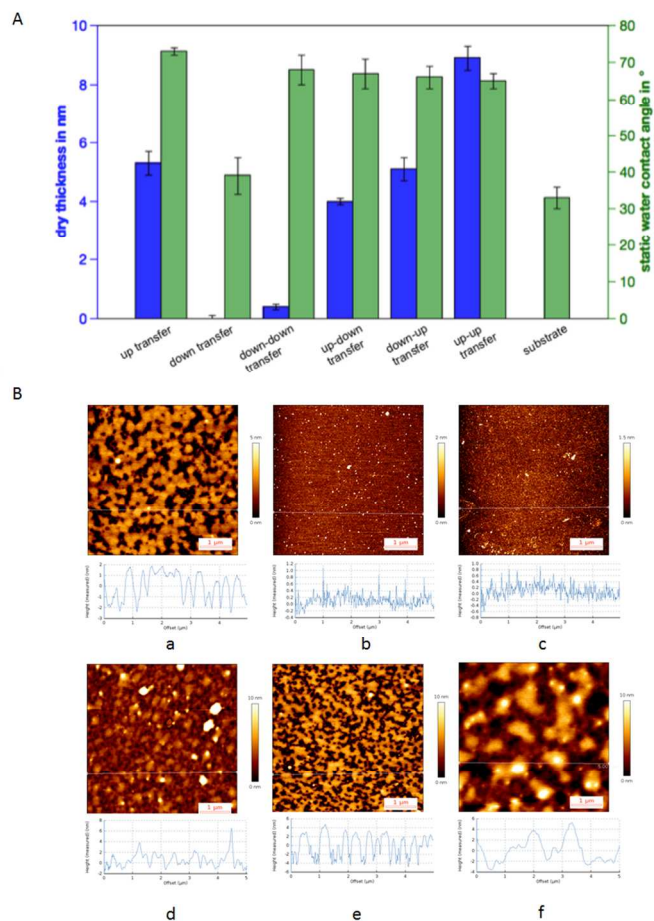


Figure 2. LB transfers to generate the polymer films: A – transfer directions (a – down transfer, down deeping; b – up transfer, up lifting; c – up-down transfer; d – down-up transfer; e – down-down transfer; f – up-up transfer); B – films resulting from specific transfers (a – monolayer film; b – bilayer film).

224x117mm (96 x 96 DPI)



45 Figure 3. Characterization of different solid supported A45-B101-C27 copolymer films: A – thickness and
46 wettability; B – AFM images (AC mode in air) with different transfer types and their height profiles (a – up
47 transfer, monolayer film formed; b – down transfer, no film formation; c – down-down transfer, no film
48 formation; d – down-up transfer, down-up monolayer film formed; e – up-down transfer, up-down
49 monolayer film formed; f – up-up transfer, bilayer film formed).

50 248x398mm (96 x 96 DPI)

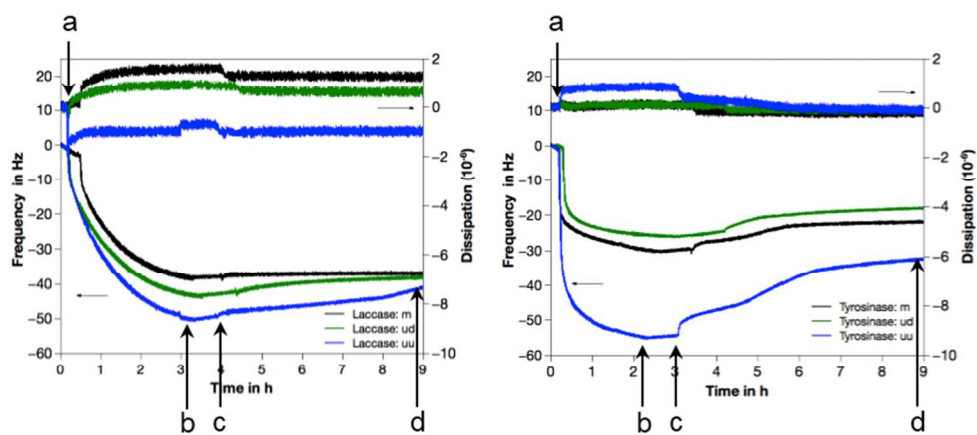


Figure 4. Changes in frequency (mass) and dissipation during the adsorption-incubation-desorption of laccase (left) and tyrosinase (right). Stages of enzymes adsorption: a – system stabilization (buffer flow); b – enzyme adsorption (enzyme flow); c – enzyme incubation (no flow); d – enzyme desorption (buffer flow). Both enzymes (0.5 $\mu\text{g mL}^{-1}$) adsorbed on polymer membranes: monolayer (m); up-down monolayer (ud) or bilayer (uu). QCM graphs were registered from the 5th overtone.

230x107mm (96 x 96 DPI)

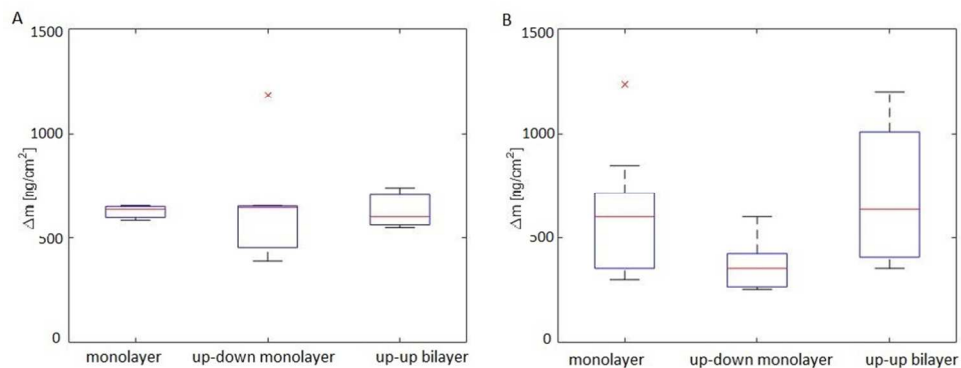


Figure 5. Amount of laccase (A) and tyrosinase (B) in ng/cm² calculated from QCM-D and shown in a boxplot with n=3-6.

291x111mm (96 x 96 DPI)

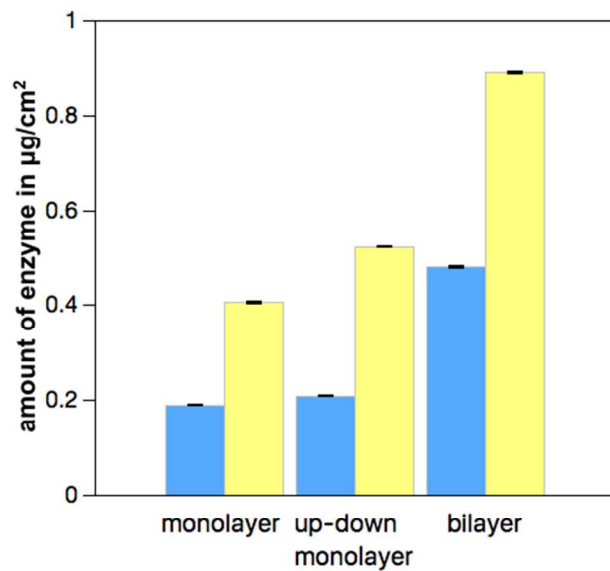


Figure 6. Amounts of laccase (blue) and tyrosinase (yellow) removed from the monolayer, up-down monolayer and bilayer polymer films, measured by BCA assay. The determined mass of the enzymes were expressed as mass per surface area ($\mu\text{g cm}^{-2}$).

270x179mm (72 x 72 DPI)

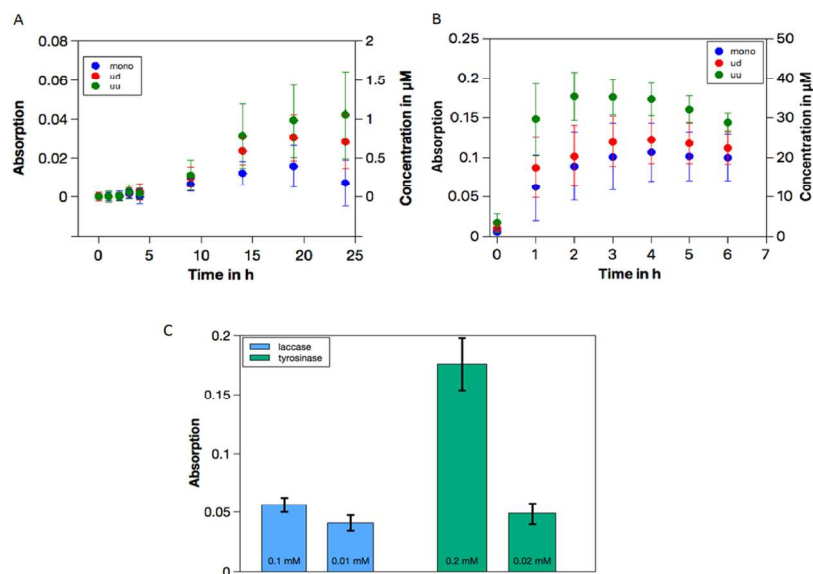
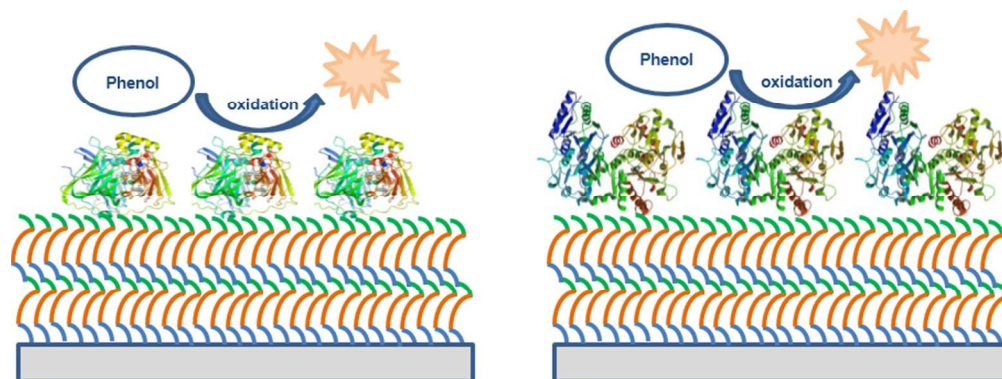


Figure 7. Activity of enzymes immobilized on the A45-B101-C27 block copolymer films as determined by oxidative product formation. (A) Laccase with 0.1 mM DMP as substrate which forms a product with a characteristic UV/vis absorption ($\lambda = 470$) (A), and (B) tyrosinase with 0.2 mM 4-MP as substrate forming a product that can be detected by UV/vis absorption at $\lambda = 492$). Curves are based on: monolayer (m, blue), up-down monolayer (ud, red), bilayer (uu, green), (lines added to guide the eye only). Activity of tyrosinase and laccase immobilized on the bilayer (uu) for two different concentrations of the enzyme substrates (C): DMP 0.1 mM and 0.01 mM (after 24 h), and 4-MP 0.2 mM and 0.02 mM (after 3 h). Enzymatic activity is shown via absorption intensity as measured and product concentration (μM) as calculated using the calibration curves in Figure S6. For all measurements, background correction has been performed by subtraction of the absorption intensity obtained when the enzyme substrate was added to the polymer membrane.

262x167mm (150 x 150 DPI)



TOC image

240x89mm (96 x 96 DPI)

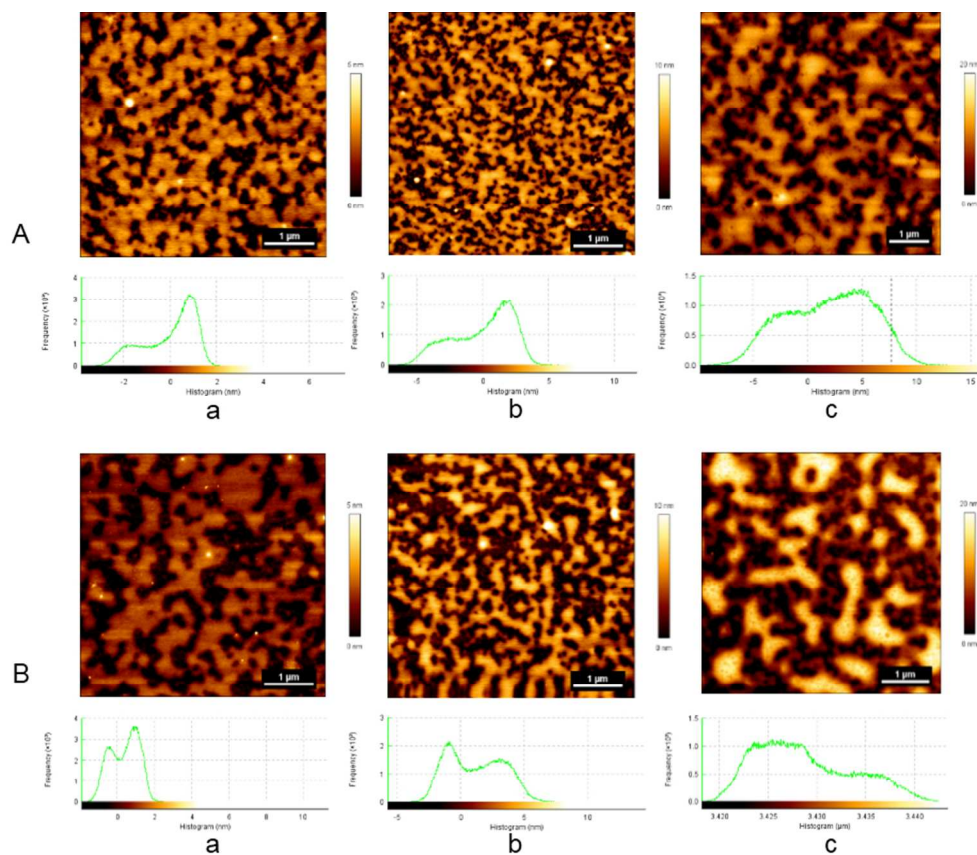
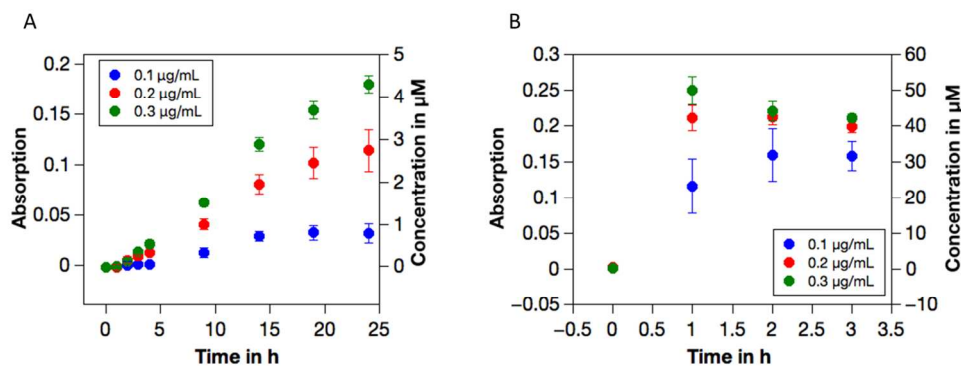


Figure S1. AFM images of the triblock copolymer film and the related histograms of the channel values: A – after 1 week; B – after 3 months; a – monolayer film; b – up-down monolayer film; c – bilayer film.

248x214mm (96 x 96 DPI)



Caption : Figure S4. Activity of free (f) laccase (A) in the presence of DMP as substrate and tyrosinase (B) in the presence of 4-MP as substrate with different enzyme concentrations: 0.1 $\mu\text{g mL}^{-1}$ (blue), 0.2 $\mu\text{g mL}^{-1}$ (red), 0.3 $\mu\text{g mL}^{-1}$ (green). The activity is shown as absorption intensity (left) and as product concentration (μM , right). The product concentration was calculated using the calibration curves shown in Figure S6

427x169mm (96 x 96 DPI)

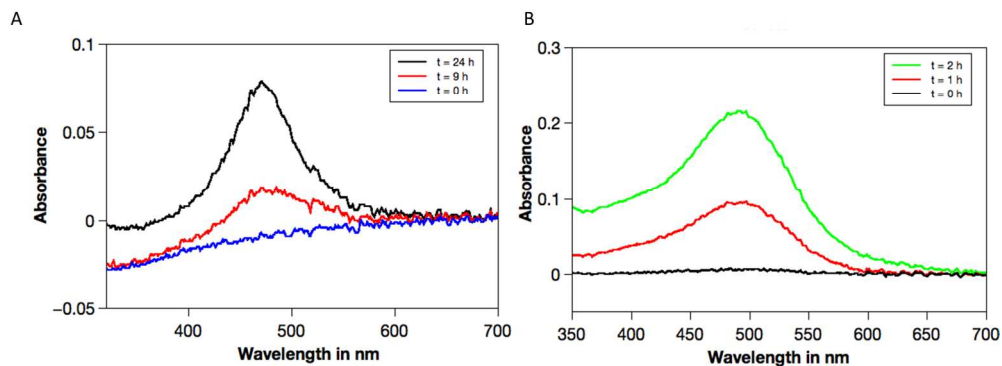


Figure S5. Absorption curves (raw data) of A) laccase with DMP (0.1 mM) and B) tyrosinase with 4-MP (0.2 mM) on up-up bilayer showing the change in peak intensity over reaction time due to product formation.

493x186mm (96 x 96 DPI)

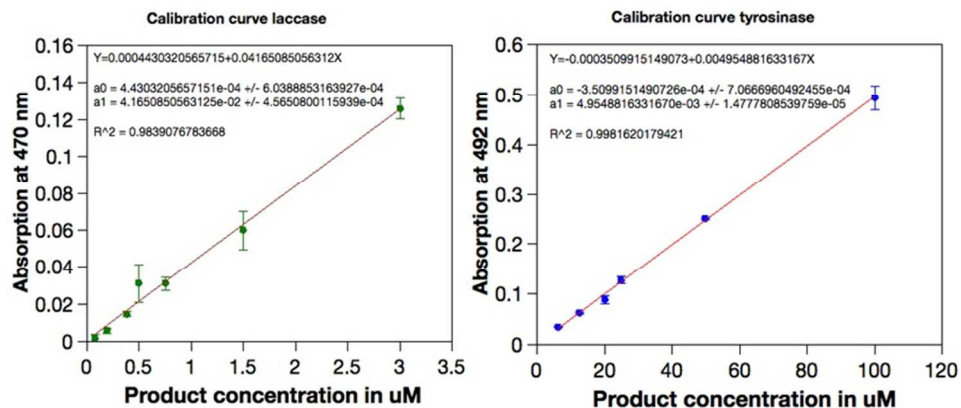


Figure S6. Calibration curves for enzymatic reactions. Left: Conversion of DMP by laccase , Right: Conversion of 4-MP and subsequent reaction with MBTH by Tyrosinase.

159x69mm (150 x 150 DPI)

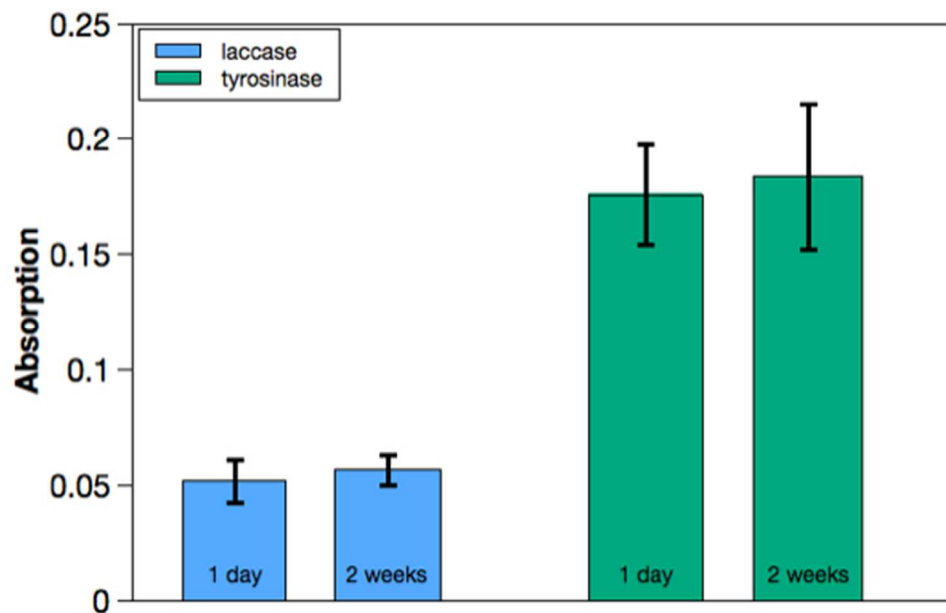


Figure S7. Activity of enzymes immobilized on the A45-B101-C27 block copolymer bilayer films with two weeks difference in preparation; laccase (blue) measured after 24 h with DMP as substrate (0.1 mM), $\lambda_{\text{max}} = 470$ nm, tyrosinase (green) measured after 3 h with 4-MP as substrate (0.2 mM), $\lambda_{\text{max}} = 492$ nm; averages of four measurements were used; error bars give standard deviation. The dispersity of the values for the immobilized enzymes activity are due to several factors: polymer transfer on the silica support, enzyme adsorption onto the polymer film, type of enzyme and substrate.

165x125mm (96 x 96 DPI)

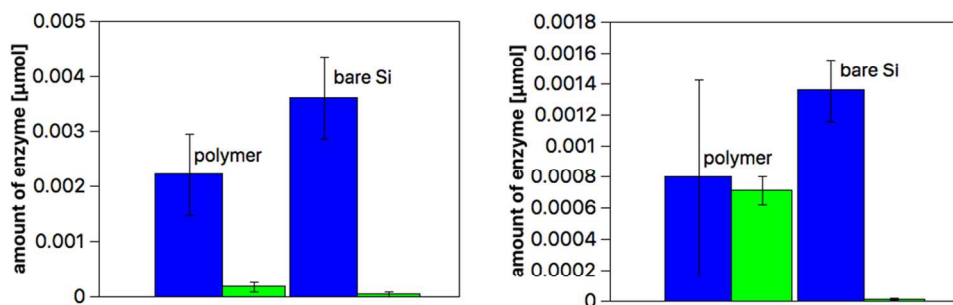


Figure S8. Determination of relative enzymatic activity of the enzymes laccase (left) and tyrosinase (right) on the bilayer polymer membrane (up-up) and on bare silicon wafer for comparison. The amount of enzyme on surface (blue) was calculated by subtracting the enzymatic activity determined in wash solutions from the washing solution used for immobilization. Hence, the remainder is assumed to be adsorbed on the surfaces. The result is compared to the experimentally determined result (green).

341x143mm (96 x 96 DPI)